Journal of Applied Electrochemistry **34**: 929–933, 2004.

Direct methanol fuel cells using thermally catalysed Ti mesh

CHAN LIM*, K. SCOTT, R.G. ALLEN and S. ROY
Department of Chemical Engineering and Advanced Materials, University of Newcastle upon Tyne, Merz Court, Newcastle upon Tyne NE1 7RU, UK
*(*author for correspondence, fax: +44-191-222-5292, e-mail: chan.lim@ncl.ac.uk)*

Received 6 January 2004; accepted in revised form 14 April 2004

Key words: catalyst, direct methanol fuel cell, mesh, Pt–Ru, thermal decomposition

Abstract

Characterisation of a direct methanol fuel cell using an anode fabricated by thermal decomposition from Pt–Ru chloro-complex on Ti mesh is described. The polarisation characteristic of the resultant membrane electrode assembly is compared with that of a conventional MEA with an anode, consisting of a catalyst layer, a microporous layer and a wet-proof-treated carbon paper. Electrode characterisation was carried out using XRD, SEM and EDX analyses. In 1 M methanol solution, the MEA with the catalysed Ti mesh anode gave a power performance comparable with that of the conventional anode at 90 °C. However, in 0.5 M methanol solution the former showed much higher power density than the latter, indicating high utilisation of methanol fuel.

1. Introduction

The direct methanol fuel cell (DMFC) based on the proton exchange membrane (PEM) has been developed as a potential power source, not only for vehicular traction and static power, but also for portable electronics due to its simplicity of design. The use of a liquid fuel is attractive due to the convenience of storage, transport and supply. However, during methanol oxidation, an anode catalyst layer releases a large volume of carbon dioxide which needs to be removed effectively through a gas diffusion-backing layer (GDL). The conventional structure of the anode consists of successive layers of catalyst layer, microporous layer and either non-woven carbon paper or woven carbon cloth impregnated with carbon black and hydrophobic polymer. This structure is not ideal for gas transport and release from the electrode surface.

In previous work [1], as a result of a flow visualisation study on the DMFC anode, it was confirmed that this conventional structure was not suitable for the transport and release of carbon oxide gas from the anode and resulted in considerable hydrodynamic and mass transport limitations for methanol at the anode. These phenomena have been encountered in many electrochemical applications, e.g. water electrolysers, chloro-alkali membrane reactors and so on. To circumvent these problems using an electrode providing high mass transport limiting current, an expanded metal mesh electrode has been adopted as the substrate material in many electrochemical reactions and has been extensively studied [2–4].

Based on earlier studies [1, 5–7], a fine metal mesh was used as a substitute for the conventional GDL in the anode because its unique open structure is likely to mitigate problems related to gas bubbles inside the conventional anode. It has been reported from a series of half cell tests [8] that a Ti mesh anode catalysed by thermal decomposition showed lower anode overpotential than that of the conventional electrode of carbon supported Pt–Ru based on wet-proof-treated carbon cloth. In previous work, the characteristics of Ti mesh-supported Pt–Ru and Pt–Ru–Sn anodes have been the subject of preliminary investigations using voltammetry and electrochemical impedance spectroscopy (L.X. Yang et al., submitted for publication).

In the present work, polarisation characteristic of the MEA involving an anode fabricated by thermally catalysing Ti mesh is investigated and compared with that of a conventional anode prepared by coating a commercial Pt–Ru unsupported catalyst onto a carbon paper GDL.

2. Experimental details

A thermal decomposition method was used to directly deposit a Pt–Ru catalyst layer on Ti mesh for an anode and a spray coating technique to a cathode catalyst layer on microporous layer-coated carbon paper. As a reference, a conventional anode was fabricated also by using the spray coating technique. For both the conventional anode and the cathode, a microporous layer consisting Vulcan XC72R (Cabot) carbon black and Teflon

(33 wt % emulsion, Fluon) was coated onto a commercial 20 wt % wet-proofed carbon paper (Toray 090, E-Tek) by a gap-adjustable knife-blade, followed by drying at 100 °C and sintering at 360 °C in an air atmosphere for 30 min.

An ink for the cathode catalyst layer was made by dispersing Pt catalyst supported on carbon (60 wt. % Pt on Vulcan XC72, E-Tek) into a mixture of an appropriate amount of the Nafion solution (5 wt. % Nafion, EW: 1100, Aldrich Chemical) and isopropyl alcohol by ball-milling with zirconia beads, followed by spraying onto the microporous layer-coated carbon paper using an airbrush (Model 100 LG, Badger). This was followed by drying at 80 °C in an atmospheric air oven. The conventional anode was prepared by the same procedure as mentioned above using unsupported Pt–Ru black (HiSPEC 6000, Pt:Ru = 1:1 atomic ratio, Alfa Aesar).

The Ti mesh-based anode was fabricated by the thermal decomposition method. Firstly, a thin Ti mesh (MicroGrid, Delker Corp.) was etched in 20 wt. % HCl solution at 80 °C for 1 min, followed by washing in deionised water and drying at room temperature. The mesh was dipped into isopropyl alcohol mixture containing 0.2 M hydrogen hexachloroplatinate (IV) hydrate and 0.2 M ruthenium(III) chloride hydrate at room temperature, followed by drying at 150 °C. The coating procedure was repeated 5 or 6 times until the final weight gain reached a loading of 2 mg cm^{-2}. The mesh coated with chloro-complex precursors was then thermally decomposed at 400 °C for 1 h in air atmosphere. The thermal-decomposed Pt–Ru/Ti mesh electrode was dipped once into the Nafion solution prior to forming a MEA.

A Nafion 117 membrane (EW 1100, Dupont) was treated to a cleaning procedure consisting of soaking in 3 wt % H_2O_2 for 1 h at 80 °C, immersing in high purity deionised water, protonating in 1 M H_2SO_4 for 1 h at 80 °C, and finally immersing again in deionised water. In order to fabricate a MEA, firstly, the cathode was positioned on one side of the membrane and then hot-pressed at 125 °C for 3 min. After that, the mesh anode was positioned on the other side of the membrane and hot-pressed to complete the MEA. The MEA was installed into a single cell fixture (consisting of graphite plates with an active area of 9 cm^2) having straight parallel flow channels with a width of 1.0 mm and a depth of 1.0 mm for both the anode and cathode. A dilute methanol solution was fed to the anode inlet at a flow rate of 12 cm^3 min^{-1} by a peristaltic pump (101U/R, Watson) without pre-heating and back-pressurisation. Non-humidified, room temperature air was fed to the cathode inlet at a flow rate of 1 dm^3 min^{-1} without pre-heating and back-pressurisation.

Before measuring a polarisation curve, the MEA was preliminarily conditioned in the single cell by circulating 1 M methanol solution into the anodic compartment and, at the same time, deionised water into the cathodic compartment for 24 h (C. Lim et al., submitted for publication). The latter helped enhance the reproducibility of the polarisation behaviour of the MEA by ensuring good hydration of Nafion particles inside the cathode catalyst layer. After circulating the methanol fuel for a week, the cell current showed a variation less than 10 %. A polarisation curve was obtained by measuring cell voltages which were stabilised at least for 1 min after applying currents in the galvanostatic mode. Anode polarisation behaviour, involving ohmic voltage drops through the electrodes and the membrane, was measured in the single cell with respect to a hydrogen-evolving cathode acting as a dynamic hydrogen electrode (DHE).

3. Results and discussion

To illustrate macroscopic structural differences between a conventional electrode based on a carbon paper GDL and a Ti-mesh electrode used in this study, micrographs of the cross-section of the conventional electrode and the surface of the Ti-mesh electrode are shown in Figure 1(a) and (b), respectively. The conventional electrode in Figure 1(a) consists of a 260 μm-thick carbon paper, a 10 μm-thick microporous layer and a 30 μm-thick catalyst layer, whereas the developmental anode in Figure 1(b) has a thermal-decomposed catalyst layer deposited directly on a Ti mesh.

As the catalyst layer is coated repeatedly on the Ti mesh by thermal decomposition, it is observed that the catalyst layer partly covers the mesh opening and also contains numerous cracks which are probably introduced due to a large shrinkage in volume resulting from

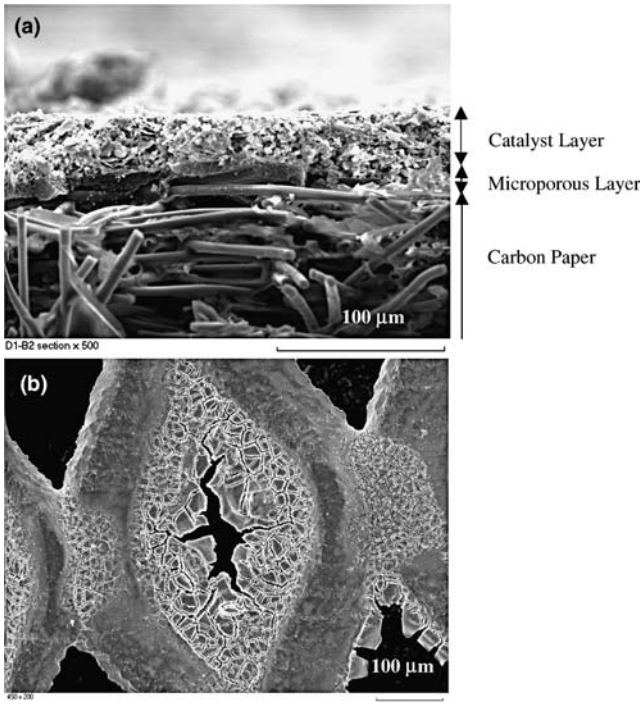

Fig. 1. SEM micrographs of macroscopic view of fuel cell anodes: (a) Pt–Ru black catalyst-coated GDL (microporous layer/Toray 090), (b) thermal-decomposed Pt–Ru on Ti mesh.

the decomposition of chlorine compounds during the period of thermal treatment. When the electrodes were used as anode for methanol oxidation in a direct methanol fuel cell, the methanol transport to the catalyst layer would be much easier in the Ti-mesh electrode as compared to the conventional electrode.

Figure 2 shows X-ray diffraction patterns (XRD) obtained from the conventional electrode (Pt–Ru black catalyst layer/microporous layer/carbon paper), thermal-decomposed Pt–Ru on the Ti mesh and a blank Ti mesh, heat-treated at 350 °C in air atmosphere, as a reference pattern from the Ti substrate. In Figure 2(a), except for the peaks at 26° and 53° in 2θ originating from graphite fibres constituting the carbon paper, the XRD pattern from the conventional electrode represented peaks of the Pt–Ru black commercial catalyst powder [9] at 40.8°, 46.7°, 69.3°, 83.4° and 87.1° in 2θ, confirming that the commercial catalyst has composed mostly of bimetallic Pt–Ru alloy particles having crystalline face-centered cubic (fcc) structure. A mean particle size was evaluated to about 4 nm from the line broadening of the (2 2 0) peaks by using the Scherrer formula [10, 11].

The thermal-decomposed catalyst layer on the Ti mesh in Figure 2(b), on the other hand, shows typical peaks of the bimetallic Pt–Ru alloy phase at 40.3°, 46.7°, 67.7°, 82.5° and 87.4° in 2θ, and interestingly peaks of β-PtO_2 and/or RuO_2 mainly represented by the peak positions at 28.2° and 35.2° in 2θ. The thermal-decomposed catalyst layer presented the peaks (2 2 0) and (3 1 1) at lower 2θ angles than the conventional Pt–Ru black catalyst layer, implying that the former has a larger lattice parameter and hence less Ru content than the latter according to Vegard's law [12]. The mean particle sizes of the Pt–Ru alloy and the oxide phase were estimated to about 5 and 34 nm by using the (2 2 0) peak of Pt–Ru alloy and the peak of oxide at 28.2°, respectively. As the peak positions of β-PtO_2 and RuO_2 are almost the same, it was not possible to discern whether the additional peaks come from β-PtO_2 or RuO_2. It might be expected that thermally decomposed Pt–Ru would have some degree of oxidation, as shown by the data.

To examine the microstructure of the catalyst layers, a cross-sectional micrograph of the conventional catalyst layer and a surface micrograph of the thermal-decomposed Pt–Ru on Ti mesh is presented in Figure 3(a) and (b), respectively. In Figure 3(a), the catalyst layer is observed on top of the microporous layer, consisting of flakes of agglomerates of Pt–Ru black which were formed by the mechanical deformation introduced during the ball milling of the catalyst ink and are reported to improve the power performance of MEA in DMFC operation (C. Lim et al., submitted for publication).

On the other hand, the thermally decomposed catalyst layer in Figure 3(b) shows a very non-homogeneous microstructure, consisting of a cracked thin film region of nano-sized particles (A), micron-sized particles (B) on top of the films, and submicron-sized particles (C) underneath the films. Considering that, in the SEM micrograph, the micron-sized particles (B) and the submicron-sized particles (C) are shown brighter than the nano-sized particles (A) in the thin film region, it is thought the particles on top of and underneath the films contain more oxides than the thin film region does, thereby giving less electron conductivity.

To determine compositional differences between the thin film region (A) and the micron-sized particles (B), energy dispersive X-ray (EDX) analyses were carried out and the results are shown in Figure 4. Although the

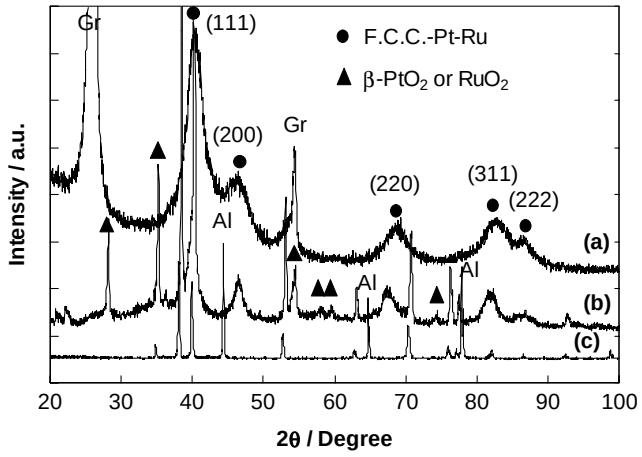

Fig. 2. XRD patterns obtained from (a) Pt–Ru black catalyst-coated GDL, (b) thermal-decomposed Pt–Ru on Ti mesh, (c) heat-treated blank Ti mesh. The A1 peaks were from a sample stage due to the open structure of Ti mesh.

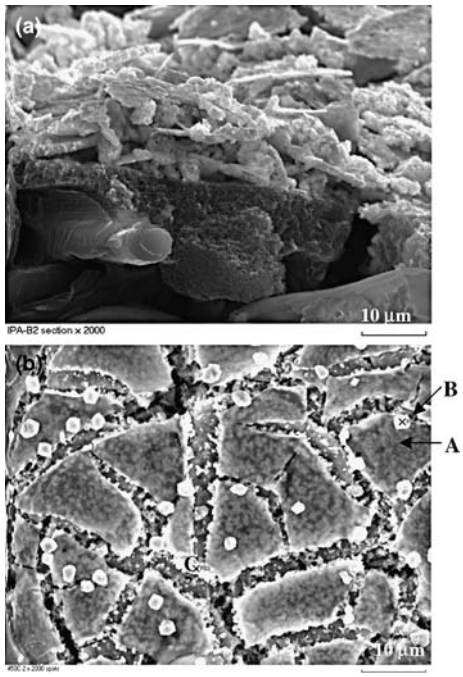

Fig. 3. SEM micrographs of anode catalyst layers prepared by (a) conventional spray coating method from ball-milled Pt–Ru black in isopropyl alcohol, (b) thermal-decomposed Pt–Ru on Ti mesh.

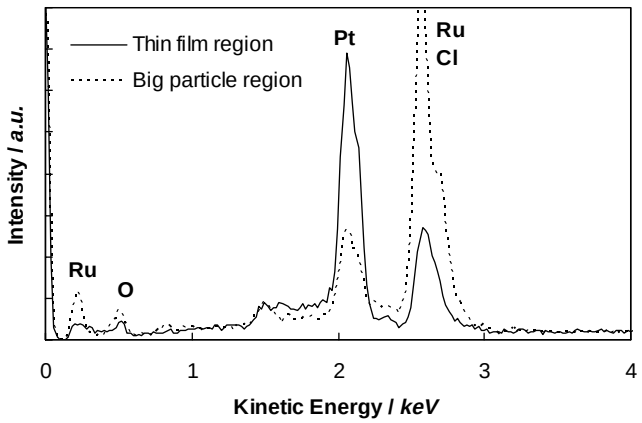

Fig. 4. EDX spectra obtained from analysis points in Figure 3(b) SEM micrograph of thermal-decomposed Pt–Ru on Ti mesh: (A) thin-film region; (B) big-particle region.

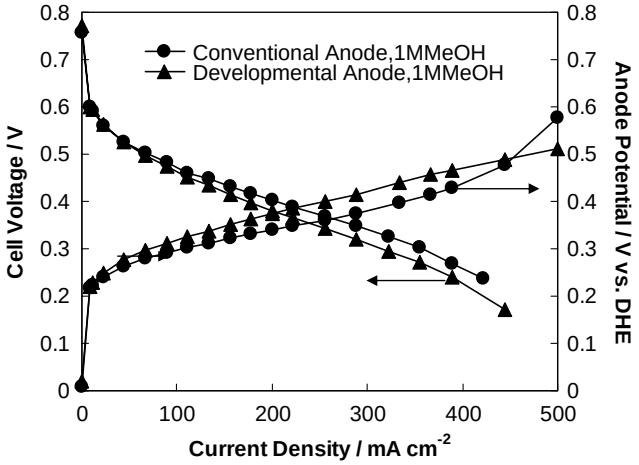

Fig. 5. Single cell voltage and anode potential vs. current density of MEAs fabricated with spray-coated conventional anode and thermal-decomposed Pt–Ru/Ti-mesh anode measured at 90 °C in 1 M CH_3OH and non-humidified atmospheric air. Anode catalyst loading was 2 mg cm^{-2} in unsupported Pt–Ru black, cathode catalyst loading 4.5 mg cm^{-2} in 60 wt.% Pt/C.

peak position of $RuL_{\alpha 1}$ (2.56 keV) is located near the peak position of $ClK_{\alpha 1}$ (2.62 keV), qualitatively, it is clearly seen, from the peaks of $RuM_{\alpha 1}$ (250 eV) and $OK_{\alpha 1}$ (525 eV), that the thin film region (A) is a Pt-rich, Ru and oxide deficient phase whereas the micron-sized particles (B) has more Ru and oxide species than the film region (A). As a result, it is thought that Ru atoms inside the thin films preferentially diffuses out of the thin film region during the heat-treatment for the thermal decomposition process, forming the micron-sized RuO_2 particles on top of the thin films as shown in Figure 3(b). The submicron-sized particles (C) underneath the thin films had almost the same Pt and Ru content as those of the thin film, except for a slightly higher oxygen content.

Cell polarisation and corresponding anode polarisation curves of the MEAs involving the carbon paper-based conventional anode or the catalysed Ti-mesh anode were evaluated in 1 M methanol solution and are presented in Figure 5. The MEA using Ti-mesh anode gives a current density of 320 mA cm^{-2} at a cell voltage of 0.3 V, comparable to that of the conventional anode (350 mA cm^{-2}) at the same cell voltage and the similar catalyst loading of 2 mg cm^{-2}. The anode polarisation vs. a dynamic hydrogen reference electrode confirmed that the MEA with the Ti mesh had a higher anode overpotential to methanol oxidation than that with the conventional electrode. This is understandable, considering that the mesh structure presents much less apparent electrode area in contact with the membrane due to the opening area of the mesh, although it is partly covered by the catalyst layer after several deposition cycles as shown in Figure 1(b). Although from XRD analysis the thermal-decomposed catalyst layer has larger particle size and less Ru content than the commercial Pt–Ru black, the mesh-based anode performed well because its open structure allows gaseous carbon dioxide to diffuse out easily from the catalyst layer and hence retains high catalyst utilisation during cell operation.

The effect of methanol concentration on the cell polarisation curves of MEAs, involving the conventional and Ti-mesh anodes are shown in Figure 6. Very interestingly, the MEA with the Ti-mesh anode maintained a performance, observed previously in 1 M methanol solution, even in 0.5 M methanol solution. At the same time, the MEA with the conventional anode was subjected to a diffusion limiting current density around 160 mA cm^{-2} much earlier than that with the developmental anode. On the other hand, in 2 M methanol solution the MEA with the developmental anode showed much lower cell voltages in the whole current regime than that with the conventional anode, indicating that the former is more vulnerable to methanol crossover than the latter.

In conclusion, the Ti-mesh anode enabled us to operate the DMFC in low molarity methanol solution without appreciable loss of performance due to its open

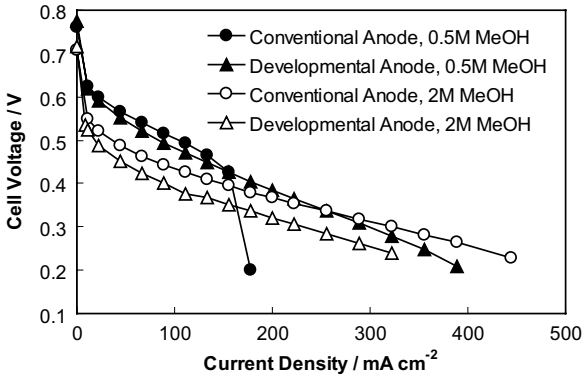

Fig. 6. Effect of methanol concentration on polarisation behaviours of MEAs with spray-coated conventional anode and with thermal-decomposed Ti-mesh anode. Data were obtained at 90 °C in non-humidified atmospheric air. Anode catalyst loading was 2 mg cm^{-2} in unsupported Pt–Ru black, cathode catalyst loading 4.5 mg cm^{-2} in 60 wt% Pt/C

structure allowing easy access of methanol to the catalyst layer. Besides the simplicity of the fabrication method of the electrode, i.e. direct formation of the catalyst layer on metal mesh by thermal decomposition, this may open up the possibility of consuming methanol efficiently in low methanol concentrations, which can reduce the methanol crossover rate through the proton conducting membrane significantly, without sacrificing performance. However, a more detailed study for methanol crossover in this new MEA configuration needs to be carried out to attain the high cell performance and fuel utilisation at the same time.

4. Conclusions

An anode for the direct methanol fuel cell has been fabricated by thermally decomposing Pt–Ru chloro-complex on Ti mesh, and the polarisation characteristics of its membrane electrode assembly have been studied in comparison with that of a conventional anode in which a catalyst layer was formed on a microporous layer-coated carbon paper by spray coating. From XRD, SEM and EDX analyses, it is believed that the thermally decomposed Pt–Ru catalyst layer on the Ti mesh consisted of partially oxidised bi-metallic Pt–Ru alloy particles and oxidised Ru-rich particles. The MEA with the Ti-mesh anode catalysed by thermal decomposition presented a power performance comparable to that with the conventional anode at 90 °C in 1 M methanol solution. The former outperformed the latter as the methanol concentration was decreased to 0.5 M because of the more open structure of the Ti-mesh-based anode, allowing easier methanol access to its catalyst layer than with the conventional anode.

Acknowledgements

UK Engineering and Physical Sciences Research Council (EPSRC) supported Dr C.L. and Miss R.G.A. as a research associate and a PhD student, respectively, during this work. The UK Ministry of Defence (MOD) supported the work through the Joint Grant Scheme, UK Defence Science and Technology Laboratory (DSTL). The work was performed in research facilities provided through an EPSRC/HEFCE Joint Infrastructure Fund (award no. JIF4NESCEQ). The supply of various metal meshes from Delker Corp. is acknowledged.

References

1. P. Argyropoulos, K. Scott and W.M. Taama, *Electrochim. Acta* **44** (1999) 3575.
2. A. Nidola, *Int. J. Hydrogen Energy* **9** (1984) 367.
3. C.J. Brown, D. Pletcher, F.C. Walsh, J.K. Hammond and D. Robinson, *J. Appl. Electrochem.* **24** (1994) 95.
4. L. Lipp and D. Pletcher, *Electrochim. Acta* **42** (1997) 1101.
5. A. Shukla, P.A. Christensen, A.J. Dickinson and A. Hamnett, *J. Power Sources* **76** (1998) 54.
6. K. Sundmacher, T. Schultz, S. Zhou, K. Scott, M. Ginkel and E.D. Gilles, *Chem. Eng. Sci.* **56** (2001) 333.
7. A.K. Shukla, C.L. Jackson, K. Scott and G. Murgia, *J. Power Sources* **111** (2002) 43.
8. H. Cheng and K. Scott, *J. Power Sources* **123** (2003) 137.
9. H.N. Dinh, X.R. Ren, F.H. Garzon, P. Zelenay and S. Gottesfeld, *J. Electroanal. Chem.* **491** (2000) 222.
10. C. He, H.R. Kunz and J.M. Fenton, *J. Electrochem. Soc.* **150** (2003) A1017.
11. A.S. Arico, P. Creti, H. Kim, R. Mantegna, N. Giordano and V. Antonucci, *J. Electrochem. Soc.* **143** (1996) 3950.
12. E. Antolini, *Mat. Chem. Phys.* **78** (2003) 563.